Tunable two-stage self-coupled optical waveguide resonators

Zhi Zou, Linjie Zhou,* Xiaomeng Sun, Jingya Xie, Haike Zhu, Liangjun Lu, Xinwan Li, and Jianping Chen

State Key Laboratory of Advanced Optical Communication Systems and Networks, Department of Electronic Engineering, Shanghai Jiao Tong University, Shanghai 200240, China

**Corresponding author: ljzhou@sjtu.edu.cn*

Received December 26, 2012; revised March 2, 2013; accepted March 5, 2013; posted March 7, 2013 (Doc. ID 182389); published April 1, 2013

We report tunable two-stage self-coupled optical waveguide (SCOW) resonators composed of a pair of mirror-imaged single SCOW resonators connected by a phase shifter in between. Experimental results show that the coupled-resonator-induced-transparency and high-order bandstop filtering characteristics can be obtained in the transmission spectra of the devices with two different configurations. The resonance spectrum can be tuned by using either a p-i-p microheater or a p-i-n diode in the phase shifter. Our theoretical modeling based on the transfer matrix method has a good agreement with the experimental results. © 2013 Optical Society of America

OCIS codes: 130.3120, 230.5750, 230.4555.

Silicon optical microresonators with high Q-factors and low modal volumes are promising building blocks for highly compact photonic integrated circuits (PICs) [1,2]. Various kinds of microresonator structures have been proposed and used in today's PICs, including microring, microdisk, photonic crystal resonators, etc. [3]. A single microresonator can be useful for a wide scope of applications, such as optical switching, filtering, buffering, and quantum information processing [4]. Cascaded microresonators also take an important role in optical signal processing owing to the coherent interference effect between microresonators [5]. In our previous work, we proposed a self-coupled optical waveguide (SCOW) resonator, in which clockwise (CW) and counter-clockwise (CCW) modes are coexcited, resulting in distinct resonance features from conventional micro-resonators [6].

In this Letter, we report our experimental demonstration of two-stage SCOW resonators and show that the coupled-resonator-induced-transparency (CRIT) and high-order bandstop filtering feature can be achieved by properly choosing the coupling coefficients of individual SCOW resonators. The corresponding resonance spectra can be tuned by changing the phase in between the SCOW resonators. CRIT, with the unique property that a narrow transparency peak residing in a broader absorption valley, can be utilized for coherent manipulation of light, including optical buffering, filtering, biosensing, switching, and routing [7,8]. On the other hand, high-order optical bandstop filters can find rich applications in wavelength division multiplexing and microwave-photonic systems [9].

Figure 1(a) shows the scanning electron microscope (SEM) image of our proposed device before clad with an insulating oxide layer. The device consists of a pair of mirror-imaged SCOW resonators connected by a phase shifter in between. As the input light can be reflected back by the SCOW resonator near its resonance wavelength, an additional Fabry–Perot (FP) resonance can be generated between the two SCOW resonators, which can couple with and consequently tailor the resonance spectrum. A variety of resonance spectra can be generated by tuning the two couplers and the phase shifter. The coupling coefficients of the two couplers determine the reflection of the SCOW resonator, and the phase shifter determines the detuning between the SCOW and FP resonances. Two types of phase shifters are used in our devices. The first one is based on a lateral p-i-p junction as shown in Fig. 1(c), where the waveguide itself works as a resistor. As the intrinsic region has high resistivity, heat will be generated when an electric current flows through the p-i-p junction. The device has a large tuning range since no extra loss is induced after heating up. The other one is based on a lateral p-i-n junction as shown in the Fig. 1(d). The refractive index of the rib waveguide is varied through the free-carrier plasma dispersion effect when a forward voltage is applied. Compared to the p-i-p microheater, the p-i-n diode is only suitable for small phase shift due to the excess optical loss induced by the injected free carriers.

We fabricated our devices using a silicon-on-insulator wafer with a 220 nm thick top silicon layer and a 2 μm thick buried oxide layer. The fabrication process for our devices has been described in our previous paper [10]. Figure 1(b) shows the microscope image of the final active device. The cross-sectional dimension of the silicon waveguide is 450 nm × 220 nm and the slab height is 60 nm. The n^+ and p^+ regions are 4 μm wide, and each has a separation of 0.6 μm from the waveguide sidewall. The bending radii of outer ring and the inner bridge waveguides are 6 and 12 μm, respectively. The length of

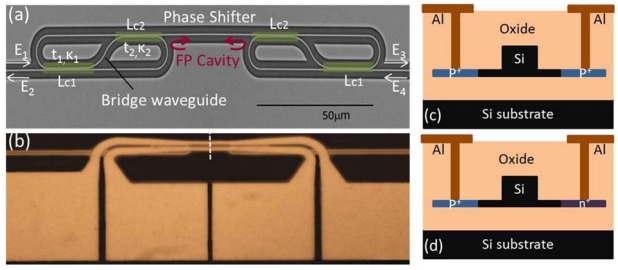

Fig. 1. (Color online) (a) SEM image of the two-stage SCOW resonators before upper-cladding. (b) Microscope image of the final active device. (c) and (d) Cross-sectional view schematics of the two phase shifters used in our devices: (c) p-i-p junction and (d) p-i-n diode.

the phase shifter is properly designed such that the round-trip length of the FP resonator doubles that of the individual SCOW resonator.

The transmission spectrum of the device is measured using the Agilent loss and dispersion analyzer (86038B). The measurements are all for transverse electric-polarization. Inverse tapers with a tip width of 180 nm are used at both ends of the devices to improve the coupling efficiency.

Figures 2(a) and 2(b) show the measured transmission spectra of the two-stage SCOW resonators with two sets of couplers (coupling lengths L_{c1} and L_{c2}) prior to tuning. The coupling gap is 200 nm. The propagation loss of the waveguides is about 3.5 dB/cm. The total (fiber-to-fiber) insertion loss is ~16 dB. When $L_{c1} = 6$ μm and $L_{c2} = 10$ μm, the transmission spectrum exhibits a CRIT peak in a 0.6 nm wide opaque valley, as shown in Fig. 2(a). The relatively wide opaque window is resulted from the coexcitation of CW and CCW modes in the individual SCOW resonators [6], which is different from the microring resonator based CRIT [5]. The full-width-half-maximum (FWHM) width of the CRIT peak is ~55 pm, corresponding to a quality (Q)-factor of 28,000. When $L_{c1} = 8$ μm and $L_{c2} = 12$ μm, the transmission spectrum exhibits a single sharp dip, as shown in Fig. 2(b). The extinction ratio of the dip is ~29 dB. The FWHM width is ~0.42 nm.

Figure 2(c) shows the evolution of the CRIT spectrum when electric current is applied to the p-i-p resistor based phase shifter. The voltage drop is in-situ monitored so that the power consumption can be recorded. It can be seen that the CRIT peak periodically moves in the opaque valley and the peak intensity become lower when it moves to the edges of the valley. Interestingly, the CRIT peak disappears when the tuning power is around 4.50 mW. Note that the opaque window is also slightly red-shifted due to the lateral diffusion of heat. From the experimental results, we see that the CRIT peak can be conveniently switched on/off by tuning the phase of the connection waveguide. Such an effect could be utilized for optical switch or routing if the optical signal is carried by the original CRIT wavelength [8].

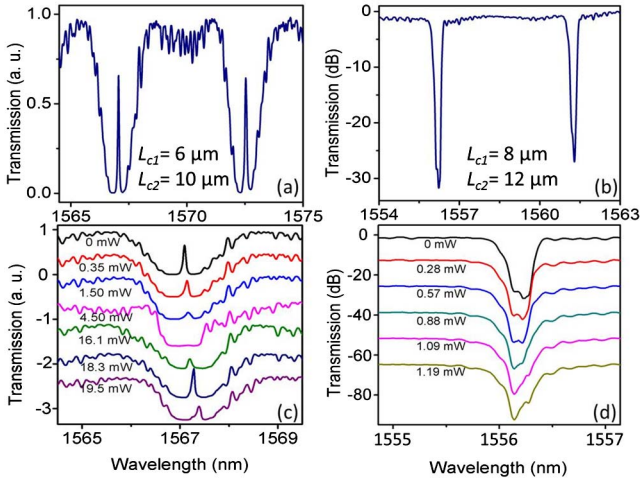

Fig. 2. (Color online) (a) and (b) Experimental transmission spectra of the two-stage SCOW resonators without tuning. (c) CRIT resonance spectra under various thermal powers. (d) High-order bandstop filtering spectra under various electrical powers. The coupling lengths in the individual resonator are (a) and (c) $L_{c1} = 6$ μm, $L_{c2} = 10$ μm, and (b) and (d) $L_{c1} = 8$ μm, $L_{c2} = 12$ μm. Curves in (c) and (d) are vertically shifted for clarity.

Figure 2(d) shows the evolution of the sharp dip with the tuning power. The phase shifter used in this device is based on a p-i-n junction. We can see that the bottom shape of the resonance dip can be actively tailored. In particular, when the tuning power is around 0.57 mW, the bottom ripple is minimized to 1.1 dB. This feature can be used to correct the fabrication induced phase error of the device working as a bandstop filter. As each SCOW resonator has CW and CCW modes coexcited, the filter constituted by the two-stage SCOW resonators is essentially a fourth-order bandstop filter.

To explain the experimental results, we use the transfer matrix method to theoretically model these devices. The field forward (backward) transmission coefficient of the individual SCOW resonators is t_{s1} (t_{s2}). Because of reciprocity, we have $t_{s1} = t_{s2}$. The reflection coefficients at the left and right ports of the first (second) SCOW resonator are r_{s1} (r_{s2}) and r_{s2} (r_{s2}), respectively. Note that r_{s1} and r_{s2} are not necessarily equal. Their analytical expressions are given by [6]

$$t_{s1} = t_{s2} = -e^{-i\theta_b}\left[\frac{(\kappa_1 - \kappa_2 a e^{-i\phi})(\kappa_2 - \kappa_1 a e^{-i\phi})}{(1-\kappa_1\kappa_2 a e^{-i\phi})^2} + \left(\frac{t_1 t_2 a^{1/2} e^{-i\phi/2}}{1-\kappa_1\kappa_2 a e^{-i\phi}}\right)^2\right], \quad (1)$$

$$r_{s1} = 2e^{-i\theta_b}\frac{t_1 t_2 a^{1/2} e^{-i\phi/2}}{1-\kappa_1\kappa_2 a e^{-i\phi}}\frac{\kappa_1 - \kappa_2 a e^{-i\phi}}{1-\kappa_1\kappa_2 a e^{-i\phi}}, \quad (2)$$

$$r_{s2} = 2e^{-i\theta_b}\frac{t_1 t_2 a^{1/2} e^{-i\phi/2}}{1-\kappa_1\kappa_2 a e^{-i\phi}}\frac{\kappa_2 - \kappa_1 a e^{-i\phi}}{1-\kappa_1\kappa_2 a e^{-i\phi}}, \quad (3)$$

where ϕ is the SCOW resonator round-trip phase shift, a is the loss factor associated with the SCOW resonator, θ_b is the phase shift associated with the bridge waveguide, and t_i and κ_i ($i = 1, 2$) denote, respectively, the transmission and coupling coefficients of the two couplers of the individual SCOW resonators.

Figures 3(a) and 3(b) show the intensity transmission and reflection spectra of a single SCOW resonator assuming the coupling coefficients are $\kappa_1^2 = 0.650$, $\kappa_2^2 = 0.890$ and $\kappa_1^2 = 0.725$, $\kappa_2^2 = 0.951$, respectively. The resonator loss factor is $\alpha = 0.988$. θ_b is set to be $(\phi - \pi)/6$. The parameters are chosen such that the modeled spectrum and its evolution could maximally agree with the experimental results. It can be seen that, with different coupling coefficients, the transmission and reflection are quite distinct, which leads to either a CRIT or a single bandstop transmission spectrum of the two-stage SCOW resonators. The light transfer through the two-stage SCOW resonators can be expressed as

$$\begin{bmatrix} E_3 \\ E_4 \end{bmatrix} = \frac{1}{t_{s1}t_{s2}t_c} \begin{bmatrix} t_{s1}t_{s2} - r_{s1}r_{s2} & r_{s1} \\ -r_{s2} & 1 \end{bmatrix} \begin{bmatrix} t_c^2 & 0 \\ 0 & 1 \end{bmatrix} \times \begin{bmatrix} t_{s1}t_{s2} - r_{s1}r_{s2} & r_{s2} \\ -r_{s1} & 1 \end{bmatrix} \begin{bmatrix} E_1 \\ E_2 \end{bmatrix}, \quad (4)$$

where E_1 (E_4) and E_2 (E_3) are the incoming and outgoing electric-fields at the left (right) end, respectively, $t_c = e^{-i(\theta_p+\Delta\theta_p)}$ is the electric-field transmission through the phase shifter, and θ_p and $\Delta\theta_p$ denote the initial phase and phase change of the phase shifter, respectively. Assuming light is only excited form the left port ($E_4 = 0$), the normalized electric-field transmission of the two-stage SCOW resonators is given by

$$\frac{E_3}{E_1} = \frac{t_{s1}t_{s2}t_c}{1 - r_{s2}^2 t_c^2}. \quad (5)$$

Figure 3(c) shows the intensity transmission spectrum of the two-stage SCOW resonators when $\Delta\theta_p = \pi/2$ is introduced to the phase shifter. θ_p is set to be $(\phi - \pi)/3$. The individual SCOW resonator parameters are corresponding to Fig. 3(a). The presence of the sharp CRIT peak in the transmission spectrum suggests that the SCOW and FP resonances are coincident [6]. The CRIT peak is due to resonant tunneling via the FP resonance. Figure 3(e) analyzes the effect of detuning between the FP and SCOW resonances. Only the evolution of the CRIT peak is shown for clarity. $\Delta\theta_p$ is chosen to correlate with the tuning power used in Fig. 2(c). We can see that the CRIT peak periodically moves (with a period of $\Delta\theta_p = \pi$) in the opaque valley with the tuning phase. When it moves toward the edges of the valley, the CRIT peak screws and the peak intensity reduced. When $\Delta\theta_p$ is far from 0.5π, for example, $\Delta\theta_p = 0.37\pi$ and 0.63π, which means the SCOW and FP resonances shift far away from each other, the CRIT peak moves into the edges of the valley and becomes too weak to be discerned in the opaque valley. This evolution trend is in good agreement with our experimental observation in Fig. 2(c).

When the cascaded SCOW resonators are made up of the individual SCOW resonators shown in Fig. 3(b) with, $\Delta\theta_p = \pi/2$ the transmission spectrum exhibits a single sharp dip with no apparent CRIT effect, as shown in Fig. 3(d). The extinction ratio of the resonance dip is above 34 dB. This is mainly due to the extremely low on-resonance transmission (below −27 dB) of the individual SCOW resonator [see Fig. 3(b)], and hereby the FP resonance is relatively weak. Figure 3(f) shows the modeled transmission spectra under various phase shifts. It can be seen that the extinction ratio and the bottom ripple can be tailored by the phase tuning, which is also consistent with the experimental results in Fig. 2(d).

In conclusion, we presented the experimental demonstration of tunable two-stage SCOW resonators. CRIT and high-order bandstop filtering features were obtained by setting different coupling coefficients in the individual SCOW resonators. The CRIT peak wavelength and intensity can be tuned by the phase shifter, which can be used for optical switches and routers. The stopband shape of the high-order filtering spectrum can be tailored through phase tuning, which can be used to correct fabrication induced phase deviations.

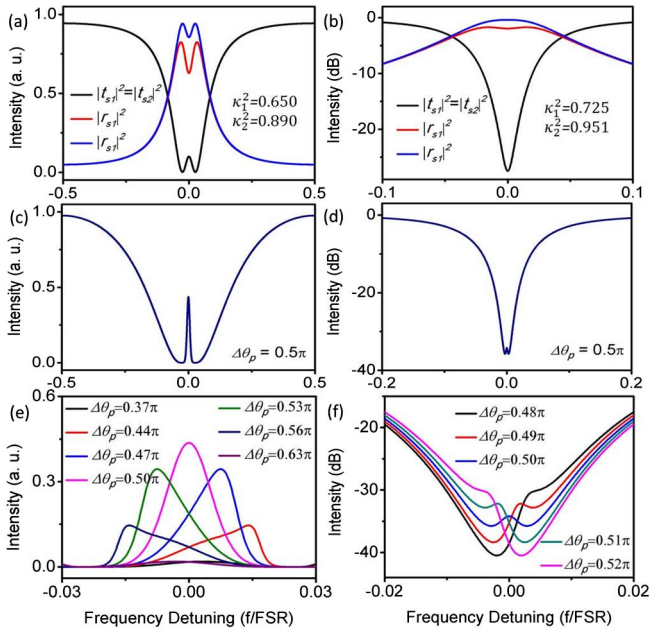

Fig. 3. (Color online) (a) and (b) Intensity transmission $|t_{S1,2}|^2$ and reflection $|r_{S1,2}|^2$ spectra of the two individual SCOW resonators. (c) and (d) Intensity transmission spectrum of the two-stage coupled SCOW resonators. The coupling coefficients in (a) and (c) are $\kappa_1^2 = 0.650$, $\kappa_2^2 = 0.890$ and in (b) and (d) $\kappa_1^2 = 0.725$, $\kappa_2^2 = 0.951$. (e) CRIT spectra and (f) high-order bandstop filtering spectra under various phase shifts. FSR is the free spectral range of the SCOW resonator.

This work was supported in part by the 973 program (ID2011CB301700), the National Natural Science Foundation of China (NSFC) (61007039, 61001074, 61127016), and the Science and Technology Commission of Shanghai Municipality (STCSM) Project (10DJ1400402, 12XD1406400). We also acknowledge IME Singapore for device fabrication.

References

1. W. Bogaerts, P. De Heyn, T. van Vaerenbergh, K. De Vos, S. Kumar Selvaraja, T. Claes, P. Dumon, P. Bienstman, D. van Thourhout, and R. Baets, Laser Photon. Rev. **6**, 47 (2012).
2. S. Feng, T. Lei, H. Chen, H. Cai, X. Luo, and A. W. Poon, Laser Photon. Rev. **6**, 145 (2012).
3. K. J. Vahala, Nature **424**, 839 (2003).
4. J. Heebner, R. Grover, and T. Ibrahim, *Optical Microresonators: Theory, Fabrication, and Applications* (Springer, 2008).
5. Q. Xu, S. Sandhu, M. L. Povinelli, J. Shakya, S. Fan, and M. Lipson, Phys. Rev. Lett. **96**, 123901 (2006).
6. L. Zhou, T. Ye, and J. Chen, Opt. Lett. **36**, 13 (2011).
7. A. Naweed, G. Farca, S. I. Shopova, and A. T. Rosenberger, Phy. Rev. A **71**, 043804 (2005).
8. M. Mancinelli, P. Bettotti, J. M. Fedeli, and L. Pavesi, Opt. Express **20**, 23856 (2012).
9. M. S. Rasras, K. Tu, D. M. Gill, Y. Chen, A. E. White, S. S. Patel, A. Pomerene, D. Carothers, J. Beattie, M. Beals, J. Michel, and L. C. Kimerling, J. Lightwave Technol. **27**, 2105 (2009).
10. L. Zhou, J. Xie, L. Lu, Z. Zou, X. Sun, and J. Chen, in *Proceedings of the Conference on Asia Communication and Photonics (ACP2012)* (Optical Society of America, 2012), paper ATh4B.